OL Organic Letters

pubs.acs.org/OrgLett Letter

Radially Oriented [*n*]Cyclo-*meta*-phenylenes

Edison Castro,[†] Saber Mirzaei,[†] and Raúl Hernández Sánchez*

Cite This: https://dx.doi.org/10.1021/acs.orglett.0c03765 Read Online

ACCESS | Metrics & More | Article Recommendations | Supporting Information

ABSTRACT: Molecular compounds with zigzag carbon nanotube geometries are exceedingly rare. Here we report the synthesis and characterization of carbon-based nanotubes with zigzag geometry, best described as radially oriented [*n*]cyclo-*meta*-phenylenes, extending the tubularene family of compounds. By the incorporation of edge-sharing benzene rings into the tubularene's radial π-surface, we have uncovered the first step to give rise to the emergence of radial orbital distribution in zigzag nanorings.

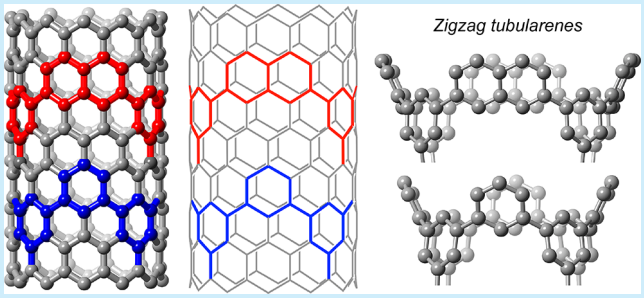

The matchless feature of carbon nanotubes (CNTs)[1] is their permanently oriented radial π-system.[2] Molecules with a rigid conformation able to display an electron cloud in this geometry were, until recently, unprecedented in the literature. The first molecule of this kind, referred to as a carbon nanobelt (CNB), comprises a "closed loop of [twelve] fully fused edge-sharing benzene rings" in an armchair[3] CNT geometry.[4] To date, few other fully fused compounds have been reported, including chiral species.[5] All reported CNBs thus far are obtained by first establishing the overall backbone connectivity in the form of an arene−alkene macrocycle or [*n*]cyclo-*para*-phenylene ([*n*]CPP),[6] which, in turn, are closed into a CNB by inducing a cascade of nickel-mediated aryl−aryl[4,7] or Scholl cyclodehydrogenation[5c] reactions, respectively. Most importantly, extrapolating a similar stepwise design logic to zigzag CNTs has not been successful (Figure 1a), although, by following other synthetic routes, zigzag CNBs have been reported.[8] Whereas [*n*]CPPs serve as nanobelt precursors for armchair geometries,[5c] related [*n*]cyclo-*meta*-phenylenes ([*n*]-CMPs)[9] could hypothetically similarly serve to synthesize zigzag-type CNBs, also termed [*n*]cyclacenes. However, [*n*]CMPs lack a radial π-system because their 1,3 connectivity favors flat macrocycles.[10] Aside from previous attempts,[11] the synthesis and characterization of radially oriented [*n*]CMPs remain largely unknown.

Recently, our group reported the synthesis of tubularenes by following an approach that facilitates the formation of the strained aromatic, the bottleneck step,[12] in a one-pot eight-fold C−C bond formation via Suzuki−Miyaura cross-coupling reaction (Figure 1b).[13] The upper rim of our previous tubularenes follows an armchair CNT geometry. Taking advantage of our modular strategy, we were able to almost double the heights of these new tubularenes **1** and **2** relative to the previous ones, at the same time allowing us to switch to a zigzag-like geometry that resembles a radially oriented [*n*]CMP. Herein we report tubular[4,12,0,8]arene (**1**) and tubular[4,16,0,12]arene (**2**), building on our prior strategy by introducing a belt of hydrogen bonds[14] to maintain the aryl reacting fragments close to each other and demonstrating the modularity of our templated approach to both armchair and zigzag CNT geometries.

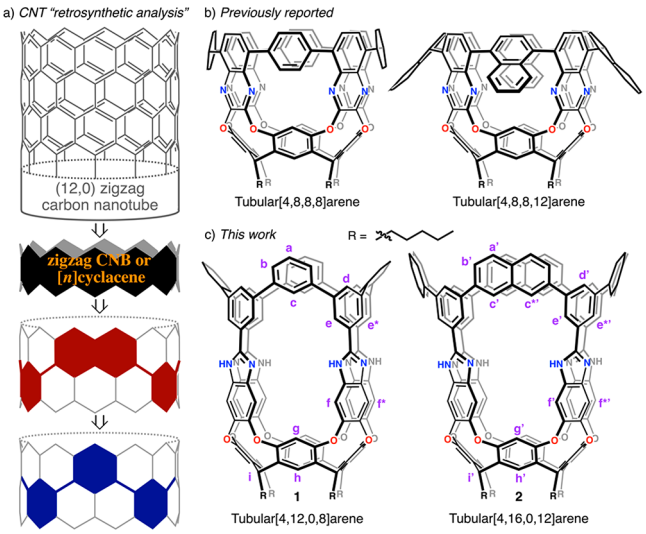

Figure 1. (a) Hypothetical retrosynthesis of zigzag CNT. (b) Previously reported armchair tubularenes with armchair connectivity. (c) Tubularenes **1** and **2** are reported herein.

Received: November 12, 2020

Abundant literature exists on the synthesis of species similar to **4**.[15] Treatment of **4** with 3,5-dibromobenzaldehyde in 4:1 EtOH/H_2O and excess $NaHSO_3$ under reflux for 2 days affords **3** in 70% yield (>2.5 g, Scheme 1). Suzuki–Miyaura

Scheme 1. Syntheses of Tubular[4,12,0,8]arene (1) and Tubular[4,16,0,12]arene (2)

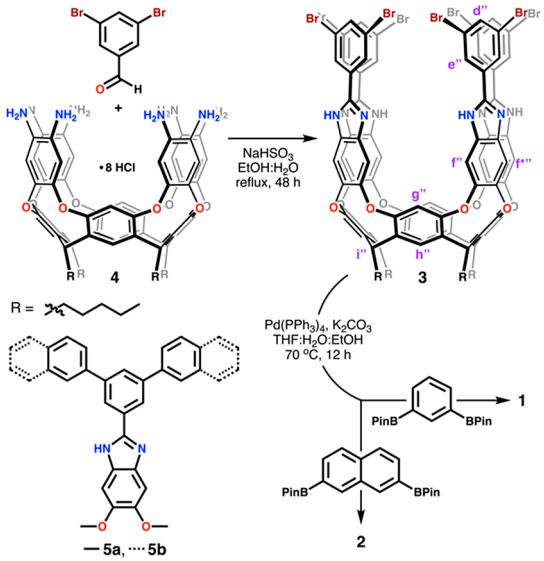

cross-coupling reaction of **3** with 1,3-phenyldiboronic acid bis(pinacol) ester in 10:1:1 THF/H_2O/EtOH at 70 °C, with excess K_2CO_3 and using $Pd(PPh_3)_4$ as a catalyst, affords **1** in a 3.3% yield. Under similar reaction conditions, the cross-coupling of **3** with 2,7-naphthalenediboronic acid bis(pinacol) ester provides **2** in 2.5% yield. Unassigned ^{1}H NMR resonances in **1** and **2** may indicate the trapping of molecules in their cavities. Analogous tubularene wall structures **5a** and **5b** (Scheme 1) were synthesized to gain more insight into the effects of rigidifying the overall architecture while maintaining the radially oriented π-system

Compounds **1**–**3** have poor solubility in standard organic solvents, but upon the addition of a small alcohol, for example, MeOH or EtOH, these species readily go into solution. Vapor diffusion of Et_2O into a solution of **3** in MeOH/DCM formed colorless block-shaped crystals. The molecular crystal structure of **3**, shown in Figure 2a, confirms our hypothesis in which a belt of hydrogen bonds is formed by the benzimidazole fragments and an external hydrogen bond donor–acceptor. Crystals of two different adducts have been obtained: **3**·2H_2O·2MeOH (Figure 2a) and **3**·H_2O·3MeOH (Figure S1). Density functional theory (DFT) optimized structures of tubularenes **1** and **2** at the MN15/6-31G*+PCM(CH_2Cl_2) level of theory are shown in Figure 2b,c, respectively. Attempts to grow crystals of **1** and **2** have only produced microcrystals with extremely weak X-ray diffraction. The structural information suggests that compounds **1**–**3** should be C_4-symmetric in solution. Indeed, ^{1}H NMR indicates a symmetric environment in all three cases (Figure 2d). From compound **3**, we expect six unique chemical aromatic environments, all integrating for one hydrogen atom, except one, **e**′′, which is expected to integrate for two hydrogen atoms. The single resonance for **e**′′ at 7.82 ppm demonstrates that at room temperature there is no steric hindrance for free rotation of the 1,3-dibromophenyl fragment, as shown in Figure 2d. Note, however, that the tubular conformer is maintained in solution, as indicated from the chemical shift of **i**′′ (>5.5 ppm, independent of the solvent system used).[16] Following a similar analysis, under C_4 symmetry we expect 10 aromatic resonances for tubularene **1** (Figure 1c). Indeed, all resonances are observed and assigned based on comparisons to **3**, DFT-calculated ^{1}H NMR (Table S4), and their splitting pattern, for example, **a** and **b**. Whereas the ^{1}H NMR of **2** is more complex relative to **1**, the long-range coupling ^4J observed in **2** helped us deduce the resonances coming from **a**′ to **e**′ (Figure 2d, Figure S13, and Table S5). Also, the MALDI-TOF MS for **1**–**3** display a single ion in each case across a wide range of m/z (Figure 2e). Upon close inspection, the observed mass spectra match the simulated $[M + H]^+$ isotopic distribution patterns for **1**–**3**, as indicated in Figure 2e1–e3.

Tubularene's rigidity is particularly relevant to maintain the radial orientation of the π-system, and it also creates a permanent cavity. Octabromo species **3** maintains its tubular shape thanks to its belt of hydrogen bonds (Figure 2e, inset). Closely related cavitands are known to flip between open (kite) and closed (vase) conformers depending on the guest or temperature,[17] and in some, the closed conformer has been enforced by intramolecular hydrogen bonding.[14b,18] Octabromo species **3** has eight hydrogen bonds formed between N and O atoms at an average distance of 2.77(1) Å (Figure S1), which is relatively short and likely provides a significant energetic stabilization to the tubular form of **3**.[19] In the absence of the hydrogen bond donor–acceptor interaction, compound **3** lacks any significant solubility, presumably forming aggregates without an internal cavity. This is not the case in **1** and **2**, where covalent bonding rigidifies the overall structure creating pores along the walls (Figure S22) and permanent internal void spaces (Figure 2e, inset). The diameters of **1** and **2** are ∼9.5 and ∼12.7 Å (Figures S23 and S24), respectively. These are remarkably larger than those of initially reported porous organic cages[20] and on par with those of state-of-the-art organic moisture-stable porphyrin box cages with permanent porosity.[21] The calculated internal volumes of **1** and **2** are ∼620 and ∼910 Å^3 (Figures S23 and S24), respectively, and were obtained in a similar way to tubular[4,8,8,8]arene.[13] Tubularene's internal cavity and rigidity make them ideal candidates for novel porous organic solids.[22]

Radially bending the aromatic π-system in **1** and **2** inherently builds strain. DFT calculations employing the homodesmotic reactions described in Figure S25, at different levels of theory, provide average strain energies (SEs) for **1** and **2** of 42.2 and 61.9 kcal/mol (Table S6),[23] respectively. These are significantly lower in comparison with the average SEs of tubular[4,8,8,8]arene and tubular[4,8,8,12]arene at 89 and 81 kcal/mol, respectively, and substantially higher than those reported for [n]CMPs[10] (≤23 kcal/mol) and [n]cyclo-2,7-naphthylenes[24] ([n]CNAP ≤ 19 kcal/mol). The obtained SEs are counterintuitive, because in a first approximation, one would expect **2** to have less strain than **1** based on its larger diameter.[25] In fact, whereas the top nanoring in **1** resembles a radial [n]CMP,[11] the analogous nanoring in **2** with its 2,7-naphthylene moieties can be devised as a partial [n]cyclacene[26] because it has conjugated edge-sharing benzene rings, a feature extensively investigated[27] and, until very recently, unprecedented[8,28] in the literature.

Tubularene **2** can be regarded as an intermediate between a fully fused zigzag nanoring, [n]cyclacene, and a nonfused

https://dx.doi.org/10.1021/acs.orglett.0c03765
Org. Lett. XXXX, XXX, XXX–XXX

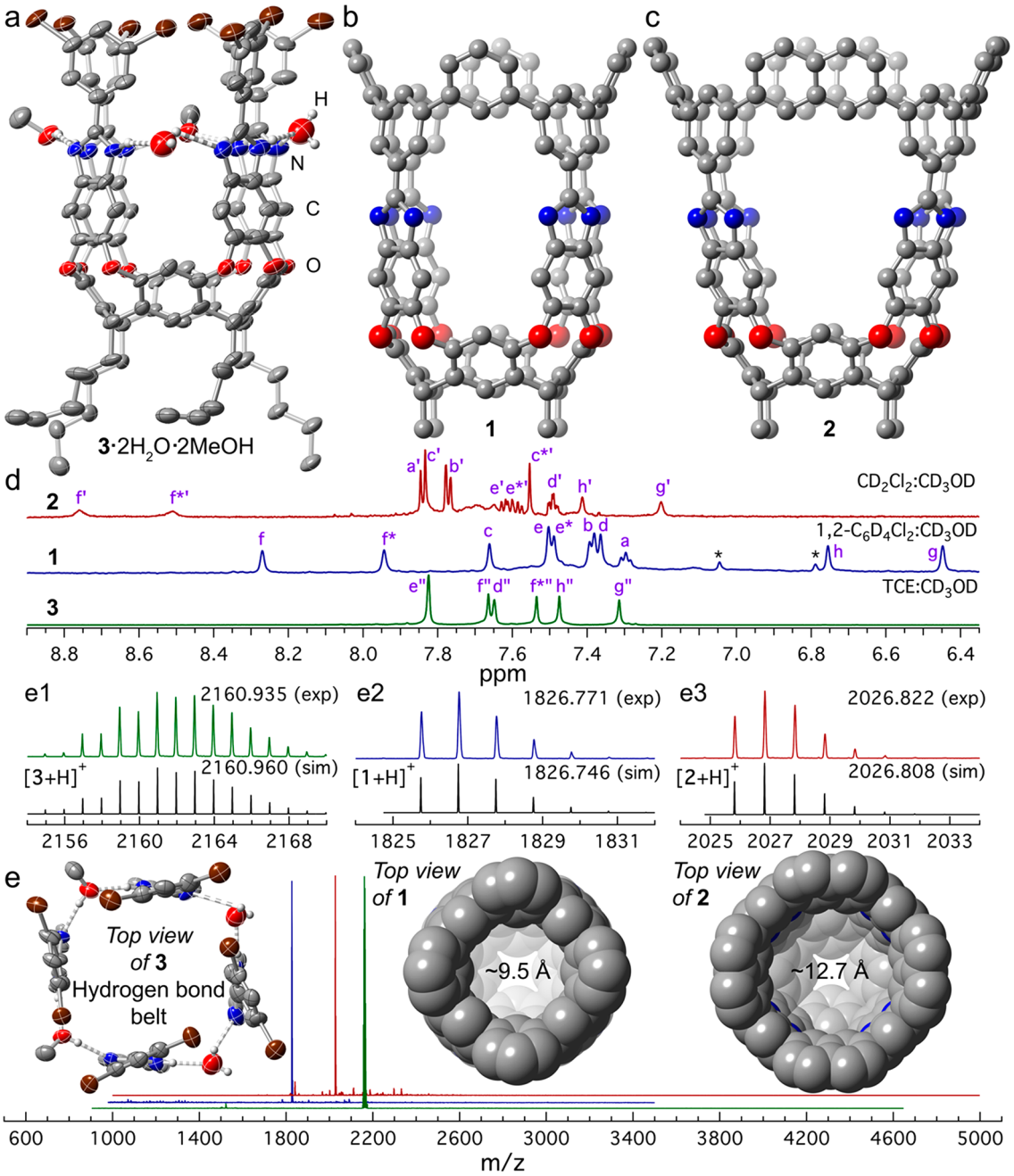

Figure 2. Characterization of **1**, **2**, and **3**. (a) Molecular crystal structure of **3**, obtained at 150 K. Thermal ellipsoids are set at 50% probability level. Hydrogen bonds are shown in stripes of white and gray. (b,c) DFT-optimized structures of **1** and **2** at the MN15/6-31G*+PCM(CH_2Cl_2) level. (d) ^{1}H NMR of **1**, **2**, and **3** in selected solvent systems. * indicates residual solvent signals from 1,2-$C_6D_4Cl_2$. (e) Experimental MALDI-TOF MS and isotope patterns of (e1) **3**, (e2) **1**, and (e3) **2**. $[M + H]^+$ simulated traces are shown in black. Insets: Top view of the structures of **1**, **2**, and **3** with their corresponding internal diameters.

radially oriented [n]CMP, just like the upper terminus in **1** (Figure 1a,c). UV−vis absorption and emission spectra of **1**−**3**, **5a**, and **5b** were collected to gain further insight into their electronic structure. The absorption bands of **1** and **2** are clearly sharper than those of their precursor **3** and the analogous wall-building block compounds **5a** and **5b** (Figure 3a). From 300 to 340 nm, an almost identical peak progression is observed with λ_{max} at [306, 317, 334] versus [305, 318, 335] nm for **1** and **2**, respectively. Note that the strong band at λ_{max} = 280 nm in **2** is the only marked difference because it is not present in **1**. Also, the absorption spectra of **1** and **2** depart significantly from those of [8]CMP[9b10] ($\lambda_{max} \approx 245$ nm) and [n]CNAP[24] (size-independent $\lambda_{max} \approx 270$ nm for n = 5−7), which only have a single broad absorption band. Time-dependent (TD) DFT calculations (Table S7) establish the HOMO-to-LUMO transition in **1** and **2** to be forbidden, akin to previous tubularenes[13] and other radially conjugated compounds.[4,29] Most importantly, absorption band sharpening is a signature of tubularene's rigidity, similar to the effects of rigidifying linear polymers,[30] and akin to a single-wall CNT.[31]

Noncontorted compounds **5a** and **5b**, analogues of the tubular walls of **1** and **2**, respectively, display two distinctive sets of two emission transitions around 370 and 470 nm (Figure 3b). Surprisingly the low-energy bands around 470 nm

https://dx.doi.org/10.1021/acs.orglett.0c03765
Org. Lett. XXXX, XXX, XXX−XXX

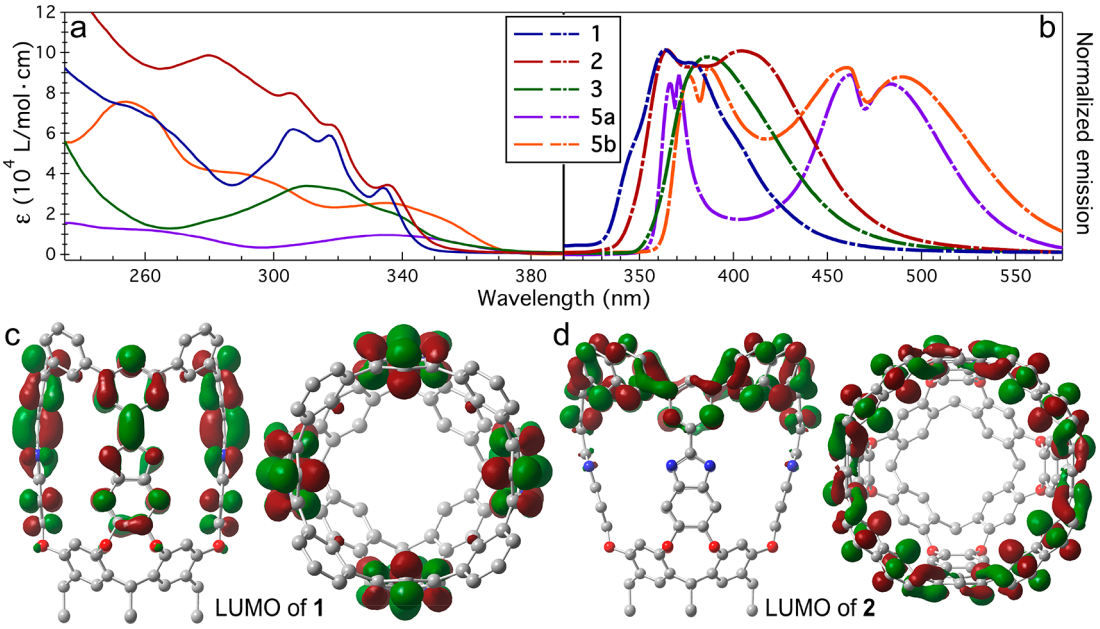

Figure 3. Electronic structure of tubularenes **1** and **2**. (a) UV−vis absorption and (b) emission spectra collected in CH_2Cl_2/MeOH (9:1) at room temperature. Emission data were collected by light excitation at 305 nm. Side and top views of LUMO density plots (±0.02 au) of tubularene (c) **1** and (d) **2**, calculated at the MN15/6-31G*+PCM(CH_2Cl_2) level of theory.

are not present in **1** and **2**, where only two peaks are observed at λ_{em} of [364, 376] nm for **1** and [365, 405] nm for **2**. Notice how the high-energy emission line is independent of the size of the zigzag nanoring in **1** and **2**, whereas the low-energy emission band red-shifts in **2**, which is likely related to its larger radial π-surface. From these optical data, an identical Stokes shift of ∼2460 cm^{-1} is observed for tubularenes **1** and **2**. This is in stark contrast with the Stokes shifts of 7065 and 6425 cm^{-1} observed in the previously reported armchair tubular-[4,8,8,8]arene and tubular[4,8,8,12]arene,[13] respectively. Compounds having large Stokes shifts, for example, >7000 cm^{-1}, are exceedingly rare,[32] and they are highly desired to prevent self-quenching of fluorophores in materials and biologically relevant applications.[33] Interestingly, when comparing zigzag to armchair tubularenes of the same diameter (∼1 nm), for example, **1** and tubular[4,8,8,8]arene, we observe a remarkable three-fold increase in the Stokes shift. Optical band gaps (E_{gap})[34] are similarly tuned between zigzag and armchair tubularenes. Whereas for **1** and **2**, we obtain 3.58 and 3.52 eV, respectively, armchair tubularenes in Figure 1b have E_{gap} values significantly smaller at ∼2.6 eV. The larger E_{gap} values in zigzag **1** and **2**, or cross-conjugated systems,[35] are attributed to their lack of global conjugation and inherent destructive quantum interference.[36] The modularity of the synthetic approach developed here, combined with our previous report,[13] demonstrates its remarkable capability to fine-tune the Stokes shifts in comparatively similar conjugated molecular nanotubes while maintaining their emissive properties, as determined from the fluorescence quantum yields (ϕ_{fl}) of 35, 39, 40, and 38% for compounds **1**, **2**, tubular[4,8,8,8]-arene, and tubular[4,8,8,12]arene (Figure S26, using anthracene as standard[37]), respectively. In comparison, note that [8]CPP and [6]CMP have poor ϕ_{fl} values of 0.084[38] and 6%,[39] respectively.

DFT calculations at different levels of theory were carried out to support the electronic structure of tubularenes **1** and **2**. Extending the radial π-surface area has a profound effect on the HOMO−LUMO density in these tubularenes (Figures S27 and S28); in fact, it is particularly evident in the LUMOs, as shown in Figure 3c,d. Whereas in **1**, the orbital density is located along its tubular walls, in **2**, the LUMO is distributed exclusively across its upper nanoring. This dramatic shift of the location of the LUMO density is also reflected in its DFT calculated energy level values, where the radially distributed LUMO of **2** is lower in energy than that of **1** across all theory levels (Table S8). Finally, the electronic structure evolution from **1** to **2** demonstrates the fundamental effect of the stepwise incorporation of edge-sharing benzene rings into zigzag nanorings en route to a fully fused system, akin to [*n*]cyclacenes.

■ ASSOCIATED CONTENT

Supporting Information

The Supporting Information is available free of charge at https://pubs.acs.org/doi/10.1021/acs.orglett.0c03765.

Experimental details; crystallographic data; ^{1}H, ^{13}C, COSY, HSQC, and HMBC NMR spectra; and DFT calculations (PDF)

Accession Codes

CCDC 2021399−2021400 and 2032615−2032616 contain the supplementary crystallographic data for this paper. These data can be obtained free of charge via www.ccdc.cam.ac.uk/data_request/cif, or by emailing data_request@ccdc.cam.ac.uk, or by contacting The Cambridge Crystallographic Data Centre, 12 Union Road, Cambridge CB2 1EZ, UK; fax: +44 1223 336033.

■ AUTHOR INFORMATION

Corresponding Author

Raúl Hernández Sánchez − *Department of Chemistry, University of Pittsburgh, Pittsburgh, Pennsylvania 15260,*

https://dx.doi.org/10.1021/acs.orglett.0c03765
Org. Lett. XXXX, XXX, XXX−XXX

United States; orcid.org/0000-0001-6013-2708; Email: raulhs@pitt.edu

Authors

Edison Castro − *Department of Chemistry, University of Pittsburgh, Pittsburgh, Pennsylvania 15260, United States;* orcid.org/0000-0003-2954-9462

Saber Mirzaei − *Department of Chemistry, University of Pittsburgh, Pittsburgh, Pennsylvania 15260, United States;* orcid.org/0000-0001-9651-9197

Complete contact information is available at: https://pubs.acs.org/10.1021/acs.orglett.0c03765

Author Contributions

†E.C. and S.M. contributed equally.

Notes

The authors declare no competing financial interest.

■ ACKNOWLEDGMENTS

We acknowledge the startup funding, the Central Research Development Fund (CRDF), and the Center for Research Computing from the University of Pittsburgh for their support. S.M. acknowledges the support from the Dietrich School of Arts & Sciences Graduate Fellowship. We thank Dr. Nathaniel J. Schuster at Stanford University for insightful discussions.

■ REFERENCES

(1) (a) Iijima, S. Helical Microtubules of Graphitic Carbon. *Nature* **1991**, *354*, 56. (b) Monthioux, M.; Kuznetsov, V. L. Who should be given the credit for the discovery of carbon nanotubes? *Carbon* **2006**, *44*, 1621.

(2) Eatemadi, A.; Daraee, H.; Karimkhanloo, H.; Kouhi, M.; Zarghami, N.; Akbarzadeh, A.; Abasi, M.; Hanifehpour, Y.; Joo, S. W. Carbon nanotubes: properties, synthesis, purification, and medical applications. *Nanoscale Res. Lett.* **2014**, *9*, 393.

(3) Saito, R.; Fujita, M.; Dresselhaus, G.; Dresselhaus, M. S. Electronic structure of chiral graphene tubules. *Appl. Phys. Lett.* **1992**, *60*, 2204.

(4) Povie, G.; Segawa, Y.; Nishihara, T.; Miyauchi, Y.; Itami, K. Synthesis of a carbon nanobelt. *Science* **2017**, *356*, 172.

(5) (a) Scott, L. T.; Jackson, E. A.; Zhang, Q.; Steinberg, B. D.; Bancu, M.; Li, B. A Short, Rigid, Structurally Pure Carbon Nanotube by Stepwise Chemical Synthesis. *J. Am. Chem. Soc.* **2012**, *134*, 107. (c) Cheung, K. Y.; Gui, S. J.; Deng, C. F.; Liang, H. F.; Xia, Z. M.; Liu, Z.; Chi, L. F.; Miao, Q. Synthesis of Armchair and Chiral Carbon Nanobelts. *Chem.* **2019**, *5*, 838. (b) Myśliwiec, D.; Kondratowicz, M.; Lis, T.; Chmielewski, P. J.; Stępień, M. Highly Strained Nonclassical Nanotube End-caps. A Single-Step Solution Synthesis from Strain-Free, Non-Macrocyclic Precursors. *J. Am. Chem. Soc.* **2015**, *137*, 1643.

(6) (a) Wu, D.; Cheng, W.; Ban, X.; Xia, J. Cycloparaphenylenes (CPPs): An Overview of Synthesis, Properties, and Potential Applications. *Asian J. Org. Chem.* **2018**, *7*, 2161. (b) Leonhardt, E. J.; Jasti, R. Emerging applications of carbon nanohoops. *Nat. Rev. Chem.* **2019**, *3*, 672.

(7) Povie, G.; Segawa, Y.; Nishihara, T.; Miyauchi, Y.; Itami, K. Synthesis and Size-Dependent Properties of [12], [16], and [24] Carbon Nanobelts. *J. Am. Chem. Soc.* **2018**, *140*, 10054.

(8) (a) Cheung, K. Y.; Watanabe, K.; Segawa, Y.; Itami, K. Synthesis of a Zigzag Carbon Nanobelt. *ChemRxiv* **2020**, DOI: 10.26434/chemrxiv.12324353.v2. (b) Chi, C.; Han, Y.; Dong, S.; Shao, J.; Fan, W. Synthesis of a Sidewall Fragment of a (12,0) Carbon Nanotube. *Angew. Chem., Int. Ed.* **2020**, DOI: 10.1002/anie.202012651.

(9) (a) Staab, H. A.; Binnig, F. Synthese Und Eigenschaften Von Hexa-Meta-Phenylen. *Tetrahedron Lett.* **1964**, *5*, 319. (b) Staab, H. A.; Binnig, F. Zur Konjugation in makrocyclischen Bindungssystemen, VII. Synthese und Eigenschaften von Hexa-m-phenylen und Octa-m-phenylen. *Chem. Ber.* **1967**, *100*, 293. (c) Cram, D. J.; Kaneda, T.; Helgeson, R. C.; Lein, G. M. Spherands - ligands whose binding of cations relieves enforced electron-electron repulsions. *J. Am. Chem. Soc.* **1979**, *101*, 6752. (d) Cram, D. J.; Kaneda, T.; Helgeson, R. C.; Brown, S. B.; Knobler, C. B.; Maverick, E.; Trueblood, K. N. Host-guest complexation. 35. Spherands, the first completely preorganized ligand systems. *J. Am. Chem. Soc.* **1985**, *107*, 3645. (e) Pisula, W.; Kastler, M.; Yang, C.; Enkelmann, V.; Müllen, K. Columnar Mesophase Formation of Cyclohexa-m-phenylene-Based Macrocycles. *Chem. - Asian J.* **2007**, *2*, 51. (f) Chan, J. M. W.; Swager, T. M. Synthesis of arylethynylated cyclohexa-m-phenylenes via sixfold Suzuki coupling. *Tetrahedron Lett.* **2008**, *49*, 4912.

(10) Xue, J. Y.; Ikemoto, K.; Takahashi, N.; Izumi, T.; Taka, H.; Kita, H.; Sato, S.; Isobe, H. Cyclo-meta-phenylene Revisited: Nickel-Mediated Synthesis, Molecular Structures, and Device Applications. *J. Org. Chem.* **2014**, *79*, 9735.

(11) André, E.; Boutonnet, B.; Charles, P.; Martini, C.; Aguiar-Hualde, J.-M.; Latil, S.; Guérineau, V.; Hammad, K.; Ray, P.; Guillot, R.; Huc, V. A New, Simple and Versatile Strategy for the Synthesis of Short Segments of Zigzag-Type Carbon Nanotubes. *Chem. - Eur. J.* **2016**, *22*, 3105.

(12) (a) Jasti, R.; Bhattacharjee, J.; Neaton, J. B.; Bertozzi, C. R. Synthesis, Characterization, and Theory of [9]-, [12]-, and [18]-Cycloparaphenylene: Carbon Nanohoop Structures. *J. Am. Chem. Soc.* **2008**, *130*, 17646. (b) Takaba, H.; Omachi, H.; Yamamoto, Y.; Bouffard, J.; Itami, K. Selective Synthesis of [12]Cycloparaphenylene. *Angew. Chem., Int. Ed.* **2009**, *48*, 6112. (c) Yamago, S.; Watanabe, Y.; Iwamoto, T. Synthesis of [8]Cycloparaphenylene from a Square-Shaped Tetranuclear Platinum Complex. *Angew. Chem., Int. Ed.* **2010**, *49*, 757. (d) Tran-Van, A.-F.; Huxol, E.; Basler, J. M.; Neuburger, M.; Adjizian, J.-J.; Ewels, C. P.; Wegner, H. A. Synthesis of Substituted [8]Cycloparaphenylenes by [2 + 2 + 2] Cycloaddition. *Org. Lett.* **2014**, *16*, 1594. (e) Huang, C.; Huang, Y.; Akhmedov, N. G.; Popp, B. V.; Petersen, J. L.; Wang, K. K. Functionalized Carbon Nanohoops: Synthesis and Structure of a [9]Cycloparaphenylene Bearing Three 5,8-Dimethoxynaphth-1,4-diyl Units. *Org. Lett.* **2014**, *16*, 2672. (f) Miyauchi, Y.; Johmoto, K.; Yasuda, N.; Uekusa, H.; Fujii, S.; Kiguchi, M.; Ito, H.; Itami, K.; Tanaka, K. Concise Synthesis and Facile Nanotube Assembly of a Symmetrically Multifunctionalized Cycloparaphenylene. *Chem. - Eur. J.* **2015**, *21*, 18900. (g) Nishigaki, S.; Shibata, Y.; Nakajima, A.; Okajima, H.; Masumoto, Y.; Osawa, T.; Muranaka, A.; Sugiyama, H.; Horikawa, A.; Uekusa, H.; Koshino, H.; Uchiyama, M.; Sakamoto, A.; Tanaka, K. Synthesis of Belt- and Möbius-Shaped Cycloparaphenylenes by Rhodium-Catalyzed Alkyne Cyclotrimerization. *J. Am. Chem. Soc.* **2019**, *141*, 14955.

(13) Mirzaei, S.; Castro, E.; Sánchez, R. H. *Tubularenes. Chem. Sci.* **2020**, *11*, 8089.

(14) (a) Far, A. R.; Shivanyuk, A.; Rebek, J. Water-stabilized cavitands. *J. Am. Chem. Soc.* **2002**, *124*, 2854. (b) Rudkevich, D. M.; Hilmersson, G.; Rebek, J. Self-folding cavitands. *J. Am. Chem. Soc.* **1998**, *120*, 12216.

(15) Mosca, S.; Yu, Y.; Rebek, J. Preparative scale and convenient synthesis of a water-soluble, deep cavitand. *Nat. Protoc.* **2016**, *11*, 1371.

(16) Roncucci, P.; Pirondini, L.; Paderni, G.; Massera, C.; Dalcanale, E.; Azov, V. A.; Diederich, F. Conformational Behavior of Pyrazine-Bridged and Mixed-Bridged Cavitands: A General Model for Solvent Effects on Thermal "Vase−Kite" Switching. *Chem. - Eur. J.* **2006**, *12*, 4775.

(17) Moran, J. R.; Ericson, J. L.; Dalcanale, E.; Bryant, J. A.; Knobler, C. B.; Cram, D. J. Vases and kites as cavitands. *J. Am. Chem. Soc.* **1991**, *113*, 5707.

(18) (a) Pochorovski, I.; Ebert, M.-O.; Gisselbrecht, J.-P.; Boudon, C.; Schweizer, W. B.; Diederich, F. Redox-Switchable Resorcin[4]-arene Cavitands: Molecular Grippers. *J. Am. Chem. Soc.* **2012**, *134*, 14702. (b) Pochorovski, I.; Milić, J.; Kolarski, D.; Gropp, C.; Schweizer, W. B.; Diederich, F. Evaluation of Hydrogen-Bond

Acceptors for Redox-Switchable Resorcin[4]arene Cavitands. *J. Am. Chem. Soc.* **2014**, *136*, 3852.

(19) Wendler, K.; Thar, J.; Zahn, S.; Kirchner, B. Estimating the Hydrogen Bond Energy. *J. Phys. Chem. A* **2010**, *114*, 9529.

(20) Tozawa, T.; Jones, J. T. A.; Swamy, S. I.; Jiang, S.; Adams, D. J.; Shakespeare, S.; Clowes, R.; Bradshaw, D.; Hasell, T.; Chong, S. Y.; Tang, C.; Thompson, S.; Parker, J.; Trewin, A.; Bacsa, J.; Slawin, A. M. Z.; Steiner, A.; Cooper, A. I. Porous organic cages. *Nat. Mater.* **2009**, *8*, 973.

(21) (a) Hong, S.; Rohman, M. R.; Jia, J.; Kim, Y.; Moon, D.; Kim, Y.; Ko, Y. H.; Lee, E.; Kim, K. Porphyrin Boxes: Rationally Designed Porous Organic Cages. *Angew. Chem., Int. Ed.* **2015**, *54*, 13241. (b) Hasell, T.; Cooper, A. I. Porous organic cages: soluble, modular and molecular pores. *Nat. Rev. Mater.* **2016**, *1*, 16053.

(22) Little, M. A.; Cooper, A. I. The Chemistry of Porous Organic Molecular Materials. *Adv. Funct. Mater.* **2020**, *30*, 1909842.

(23) The B3LYP functional without dispersion correction factors showed totally different values compared with other functionals, for example, M062X, MN15, and ωB97XD, and its own dispersion-corrected version B3LYP-D3BJ. (See the Supporting Information.) This relatively large discrepancy can be attributed to the poor simulation capabilities of B3LYP regarding noncovalent interactions (e.g., CH$-\pi$ and $\pi-\pi$) that are important in flexible molecules like **3**.

(24) Nakanishi, W.; Yoshioka, T.; Taka, H.; Xue, J. Y.; Kita, H.; Isobe, H. [n]Cyclo-2,7-naphthylenes: Synthesis and Isolation of Macrocyclic Aromatic Hydrocarbons having Bipolar Carrier Transport Ability. *Angew. Chem., Int. Ed.* **2011**, *50*, 5323.

(25) Segawa, Y.; Yagi, A.; Ito, H.; Itami, K. A Theoretical Study on the Strain Energy of Carbon Nanobelts. *Org. Lett.* **2016**, *18*, 1430.

(26) Heilbronner, E. Molecular Orbitals in homologen Reihen mehrkerniger aromatischer Kohlenwasserstoffe: I. Die Eigenwerte yon LCAO-MO's in homologen Reihen. *Helv. Chim. Acta* **1954**, *37*, 921.

(27) (a) Kohnke, F. H.; Slawin, A. M. Z.; Stoddart, J. F.; Williams, D. J. Molecular Belts and Collars in the Making: A Hexaepoxyoctacosahydro[12]cyclacene Derivative. *Angew. Chem., Int. Ed. Engl.* **1987**, *26*, 892. (b) Ashton, P. R.; Isaacs, N. S.; Kohnke, F. H.; Slawin, A. M. Z.; Spencer, C. M.; Stoddart, J. F.; Williams, D. J. Towards the Making of [12]Collarene. *Angew. Chem., Int. Ed. Engl.* **1988**, *27*, 966. (c) Ashton, P. R.; Brown, G. R.; Isaacs, N. S.; Giuffrida, D.; Kohnke, F. H.; Mathias, J. P.; Slawin, A. M. Z.; Smith, D. R.; Stoddart, J. F.; Williams, D. J. Molecular LEGO. 1. Substrate-directed synthesis via stereoregular Diels-Alder oligomerizations. *J. Am. Chem. Soc.* **1992**, *114*, 6330. (d) Schulz, F.; García, F.; Kaiser, K.; Pérez, D.; Guitián, E.; Gross, L.; Peña, D. Exploring a Route to Cyclic Acenes by On-Surface Synthesis. *Angew. Chem., Int. Ed.* **2019**, *58*, 9038. (e) Shi, T.-H.; Wang, M.-X. Zigzag Hydrocarbon Belts. *CCS Chem.* **2020**, 916. (f) Chen, H.; Gui, S.; Zhang, Y.; Liu, Z.; Miao, Q. Synthesis of a Hydrogenated Zigzag Carbon Nanobelt. *CCS Chem.* **2020**, 613.

(28) Shi, T.-H.; Guo, Q.-H.; Tong, S.; Wang, M.-X. Toward the Synthesis of a Highly Strained Hydrocarbon Belt. *J. Am. Chem. Soc.* **2020**, *142*, 4576.

(29) Lewis, S. E. Cycloparaphenylenes and related nanohoops. *Chem. Soc. Rev.* **2015**, *44*, 2221.

(30) Scherf, U.; Müllen, K. Polyarylenes and poly(arylenevinylene)s: 8. The first soluble ladder polymer with 1,4-benzoquinone-bismethide subunits. *Polymer* **1992**, *33*, 2443.

(31) (a) Blancon, J.-C.; Paillet, M.; Tran, H. N.; Than, X. T.; Guebrou, S. A.; Ayari, A.; Miguel, A. S.; Phan, N.-M.; Zahab, A.-A.; Sauvajol, J.-L.; Fatti, N. D.; Vallée, F. Direct measurement of the absolute absorption spectrum of individual semiconducting single-wall carbon nanotubes. *Nat. Commun.* **2013**, *4*, 2542. (b) Silva, J.; Oliveira, M. J. T.; Lanceros-Mendez, S.; Nogueira, F. Finite-Size Effects in the Absorption Spectra of a Single-Wall Carbon Nanotube. *J. Phys. Chem. C* **2016**, *120*, 18268.

(32) (a) Araneda, J. F.; Piers, W. E.; Heyne, B.; Parvez, M.; McDonald, R. High Stokes Shift Anilido-Pyridine Boron Difluoride Dyes. *Angew. Chem., Int. Ed.* **2011**, *50*, 12214. (b) Bogh, S. A.; Carro-Temboury, M. R.; Cerretani, C.; Swasey, S. M.; Copp, S. M.; Gwinn, E. G.; Vosch, T. Unusually large Stokes shift for a near-infrared emitting DNA-stabilized silver nanocluster. *Methods Appl. Fluoresc.* **2018**, *6*, No. 024004. (c) Luo, Y.; Hau, C.-K.; Yeung, Y. Y.; Wong, K.-L.; Shiu, K. K.; Tanner, P. A. Massive Stokes shift in 12-coordinate $Ce(NO_2)_6^{3-}$: crystal structure, vibrational and electronic spectra. *Sci. Rep.* **2018**, *8*, 16557. (d) Dhara, A.; Sadhukhan, T.; Sheetz, E. G.; Olsson, A. H.; Raghavachari, K.; Flood, A. H. Zero-Overlap Fluorophores for Fluorescent Studies at Any Concentration. *J. Am. Chem. Soc.* **2020**, *142*, 12167.

(33) (a) Shcherbakova, D. M.; Hink, M. A.; Joosen, L.; Gadella, T. W. J.; Verkhusha, V. V. An Orange Fluorescent Protein with a Large Stokes Shift for Single-Excitation Multicolor FCCS and FRET Imaging. *J. Am. Chem. Soc.* **2012**, *134*, 7913. (b) Della Sala, P.; Buccheri, N.; Sanzone, A.; Sassi, M.; Neri, P.; Talotta, C.; Rocco, A.; Pinchetti, V.; Beverina, L.; Brovelli, S.; Gaeta, C. First demonstration of the use of very large Stokes shift cycloparaphenylenes as promising organic luminophores for transparent luminescent solar concentrators. *Chem. Commun.* **2019**, *55*, 3160.

(34) Costa, J. C. S.; Taveira, R. J. S.; Lima, C. F. R. A. C.; Mendes, A.; Santos, L. M. N. B. F. Optical band gaps of organic semiconductor materials. *Opt. Mater.* **2016**, *58*, 51.

(35) Gu, J.; Wu, W.; Stuyver, T.; Danovich, D.; Hoffmann, R.; Tsuji, Y.; Shaik, S. Cross Conjugation in Polyenes and Related Hydrocarbons: What Can Be Learned from Valence Bond Theory about Single-Molecule Conductance? *J. Am. Chem. Soc.* **2019**, *141*, 6030.

(36) (a) Valkenier, H.; Guédon, C. M.; Markussen, T.; Thygesen, K. S.; van der Molen, S. J.; Hummelen, J. C. Cross-conjugation and quantum interference: a general correlation? *Phys. Chem. Chem. Phys.* **2014**, *16*, 653. (b) Li, Y.; Buerkle, M.; Li, G.; Rostamian, A.; Wang, H.; Wang, Z.; Bowler, D. R.; Miyazaki, T.; Xiang, L.; Asai, Y.; Zhou, G.; Tao, N. Gate controlling of quantum interference and direct observation of anti-resonances in single molecule charge transport. *Nat. Mater.* **2019**, *18*, 357.

(37) Williams, A. T. R.; Winfield, S. A.; Miller, J. N. Relative fluorescence quantum yields using a computer-controlled luminescence spectrometer. *Analyst* **1983**, *108*, 1067.

(38) Fujitsuka, M.; Cho, D. W.; Iwamoto, T.; Yamago, S.; Majima, T. Size-dependent fluorescence properties of [n]cycloparaphenylenes (n = 8−13), hoop-shaped π-conjugated molecules. *Phys. Chem. Chem. Phys.* **2012**, *14*, 14585.

(39) Ikemoto, K.; Tokuhira, T.; Uetani, A.; Harabuchi, Y.; Sato, S.; Maeda, S.; Isobe, H. Fluorescence Enhancement of Aromatic Macrocycles by Lowering Excited Singlet State Energies. *J. Org. Chem.* **2020**, *85*, 150.

https://dx.doi.org/10.1021/acs.orglett.0c03765
Org. Lett. XXXX, XXX, XXX−XXX